pISSN 1598-2998, eISSN 2005-9256

https://doi.org/10.4143/crt.2024.1245 Cancer Res Treat. 2026;58(2):465-480

Original Article

Anticancer Treatment Influences *TREM2* in Tumor-Associated Macrophages in Lung Cancer

Yoon Jin Cha[1], **Eun Hye Lee**[2], **Chi Young Kim**[2], **Yong Jun Choi**[2], **Min Kyung Park**[2], **Sang Hoon Lee**[2], **Eun Young Kim**[2], **Yoon Soo Chang**[2]

[1]*Department of Pathology,* [2]*Department of Internal Medicine, Yonsei University College of Medicine, Seoul, Korea*

Purpose The triggering receptor expressed on myeloid cells 2 (TREM2) creates an immunosuppressive environment, but the effects of anticancer treatment on TREM2 and the tumor microenvironment (TME) are not well established. This study investigates the impact of chemotherapy on TREM2-expressing macrophages within the lung adenocarcinoma TME.

Materials and Methods Using single-cell RNA sequencing datasets of paired normal-appearing lung tissue (NL) and tumor (Tu), human and mouse lung cancer tissue, and THP-1 cells, we observed the effects of anticancer drugs on them.

Results Myeloid cells (MY) were the second-most abundant non-epithelial component in the Tu, though less prevalent than in NL. Specific MY subclusters abundant in Tu showed overexpression of *TREM2*. In lung cancer-induced Kras-G12D mice, M2 proportion increased in Tu compared to NL; cisplatin increased TREM2+ M2 proportion in Tu. TREM2+ cells in Tu showed interactions with cell clusters showing characteristics of interstitial macrophage such as mo-lineage, mono-Mc, and CD163/LGMN cells via FN:CD44 and MIF:CD74+CXCR4, suggesting that they influence the recruitment of those cells to Tu and TME reshape. In M0-state THP-1 cells, cisplatin and osimertinib treatments induced polarization towards M1 and M2 states and increased TREM2 expression. Cisplatin promoted uptake of phosphatidylserine-coated latex beads by M0 cells, whereas osimertinib reduced uptake by polarized macrophages. These findings suggest anticancer treatments impact the lung immune microenvironment by altering the TREM2+ cells.

Conclusion Given TREM2's central inhibitory role in the tumor immune environment, effects of chemotherapeutic agents should be considered in developing TREM2-targeting therapies.

Key words Anticancer treatment, Macrophages, Tumor microenvironment, TREM2, Cisplatin

Introduction

The pivotal role of the tumor microenvironment (TME) in treating lung cancer is well-recognized. As the landscape of therapeutic options evolves, monitoring how these treatments influence the TME to enhance clinical outcomes is crucial. Macrophages, as major cellular components in both normal-appearing lung tissue (NL) and lung TME (Tu), are of particular interest. Within the TME, tumor-associated macrophages (TAMs) play a critical role, with triggering receptor expressed on myeloid cells 2 (*TREM2*) serving as an immune signaling hub that interacts with various ligands from damaged tissues, leading to natural killer (NK) cell depletion and an immunosuppressive environment [1,2]. Despite progress in delineating macrophage characteristics across different disease states, insights on how anticancer therapies modify macrophage behavior, particularly efferocytosis, are rare.

Pioneering clinical trials such as NEJ009 [3-6] and FLAURA2 [7] have demonstrated the efficacy of combination therapies over epidermal growth factor receptor tyrosine kinase inhibitor (*EGFR*-TKI) monotherapies in treating *EGFR*-mutant lung cancer; therefore, their differential impacts on macrophages within the TME should be studied. This study aimed to identify these dynamics by examining the macrophage distribution and functional states in NL and TME, focusing on TREM2 expression and its modulation in response to anticancer drugs. Our methodologies included single-cell RNA sequencing (scRNA-seq) analysis of macrophages, complemented by experimentation in cell lines and mouse and human lung cancer tissues.

Materials and Methods

1. Datasets and analytic methods

Data were analyzed using R software ver. 4.1.0 (R Foundation for Statistical Computing). Data reported by Lambrechts et al. [8], Kim et al. [9], and Cha et al. [10] were analyzed using Seurat package ver. 4.4.0. Differential gene expression (DEG) was determined using the FindMarkers function, specifying

Correspondence: Yoon Soo Chang
Department of Internal Medicine, Yonsei University College of Medicine, 63 Gil 20 Eonju-ro, Gangnam-gu, Seoul 06229, Korea
Tel: 82-2-2019-3309 E-mail: yschang@yuhs.ac
Received December 26, 2024 **Accepted** June 22, 2025 **Published Online** June 23, 2025
*Yoon Jin Cha and Eun Hye Lee contributed equally to this work.

the comparison groups for cell parameters, cells.1 and cells.2. Alluvial plots were generated using the ggalluvial package ver. 0.12.5, and pathway analysis was performed using the EnrichR package. The interactions between cell clusters were analyzed using the CellChat package ver. 1.6.1.

2. Immunohistochemistry and immunofluorescence

KrasLSL-G12D mouse lung cancer tissues treated with vehicle or cisplatin were obtained from the residual blocks of previous studies [10], which had been approved by the Institutional Animal Care and Use Committee, Yonsei Biomedical Research Institute, Yonsei University College of Medicine (2015-0307), and followed the American Association for the Assessment and Accreditation of Laboratory Animal Care guidelines. Formalin-fixed paraffin-embedded tissue blocks obtained from four mice per treatment group were used. Human tissues were randomly extracted from de-identified tissue archives of non-small cell lung cancer and institutional approval was obtained under the following number for use (IRB No. 3-2024-0207). Immunohistochemistry (IHC) was performed according to the manufacturer's instructions; the antibodies used are listed in S1 Table. Immunofluorescence (IF) was performed using the following methods. Cells or tissues were fixed with 16% methanol-free formaldehyde, blocked with 2% bovine serum albumin, and incubated with primary and secondary antibodies for 1 hour in the dark. Nuclei were stained, and slides were mounted with Fluoroshield Mounting Medium with DAPI, with images captured using a ZEISS LSM 980 confocal microscope.

3. THP-1 cell culture and polarization

THP-1 cells (human monocytic cell line) were purchased from the Korean Cell Line Bank (KCLB). A549-GFP cells (human lung carcinoma cell line expressing green fluorescent protein) were acquired from Cell Biolab Inc. (cat No. AKR-209). THP-1 cells were polarized into M0, M1, and M2 cells as described previously [11], and a schematic diagram of the process and confirmation of polarization were shown in the S2 Fig. Briefly, THP-1 cells were cultured and maintained in RPMI 1640 medium containing 10% fetal bovine serum (FBS). They were differentiated into the M0 state by treating with 150 nM phorbol 12-myristate 13-acetate (PMA; cat No. P8139, Sigma-Aldrich) for 24 hours, the M1 state by treating with 20 ng/mL IFN-γ (cat No. I17001, Sigma-Aldrich) and 10 pg/mL LPS (cat No. L6529, Sigma-Aldrich), and the M2 state by treating with 20 ng/mL human interleukin 4 (IL-4; cat No. 204-IL, R&D Systems) and 20 ng/mL IL-13 (cat No. 213-ILB, R&D Systems). The RAW 264.7 cells were cultured and maintained in Dulbecco's modified Eagle's medium (DMEM) containing 10% FBS. The M1 state was induced via treatment with 100 ng/mL LPS and 20 ng/mL mouse IFN-γ, whereas the M2 state was induced via treatment with 20 ng/mL mouse IL-4.

4. Preparation of phosphatidylserine-coated latex beads and drug treatment

Fluorescent yellow-green (cat No. L5155-1ML, Sigma-Aldrich) and fluorescent red (cat No. L3030-1ML, Sigma-Aldrich) carboxylate-modified 2 μm diameter polystyrene latex beads were used to measure the phagocytosis activity. To coat the beads with phosphatidylserine (PdSer), 99% L-α-phosphatidylserine (soy) was first dissolved in chloroform to create a 5 mM stock solution, and then the chloroform was evaporated using a rotary evaporator under reduced pressure and hypoxic condition. L-α-phosphatidylserine was then dissolved in methanol to prepare a PdSer solution, into which 50 μL of latex bead (2.4%) was added to achieve a final concentration of 0.12%. The mixture was thoroughly mixed for over 30 minutes using a Mini Lab roller Rotator (model No. H5500-230V-EU, Labnet International, Inc.), centrifuged to remove the supernatant, and the beads were resuspended in phosphate-buffered saline (PBS) for experimental use. Following drug treatment to achieve 100 nM osimertinib or 500 nM cisplatin, 20 μL/mL fluorescent red (cat No. L3030-1ML,

Table 1. Fraction of major cell population in the scRNA-seq dataset used

Cell type	Lambrechts [8]		Kim [9]		Sinjab [14]		Cha and Kim [10,15]	
	NL	Tu	NL	Tu	NL	Tu	NL	Tu
FB	2.2	3.7	4.3	4.5	4.9	11.8	2.9	7.0
EC	6.5	2.5	3.4	1.7	9.3	4.5	3.3	4.1
NK/T	48.5	59.6	45.6	51.7	42.4	21.0	40.7	44.4
BC	3.0	14.5	1.6	14.0	2.8	24.1	0.6	6.8
MA	1.5	1.3	2.8	4.8	NA[a]	NA[a]	2.7	4.7
MY	38.2	16.1	42.4	23.2	40.6	38.7	49.8	33.1

BC, B cells; EC, endothelial cells; FB, fibroblasts; MA, mast cells; MY, myeloid cells; NK/T, NK and T cells; NL, normal-appearing lung tissue; scRNA-seq, single-cell RNA sequencing; Tu, tumor. [a]In the Sinjab dataset, mast cells were included in the MY sets.

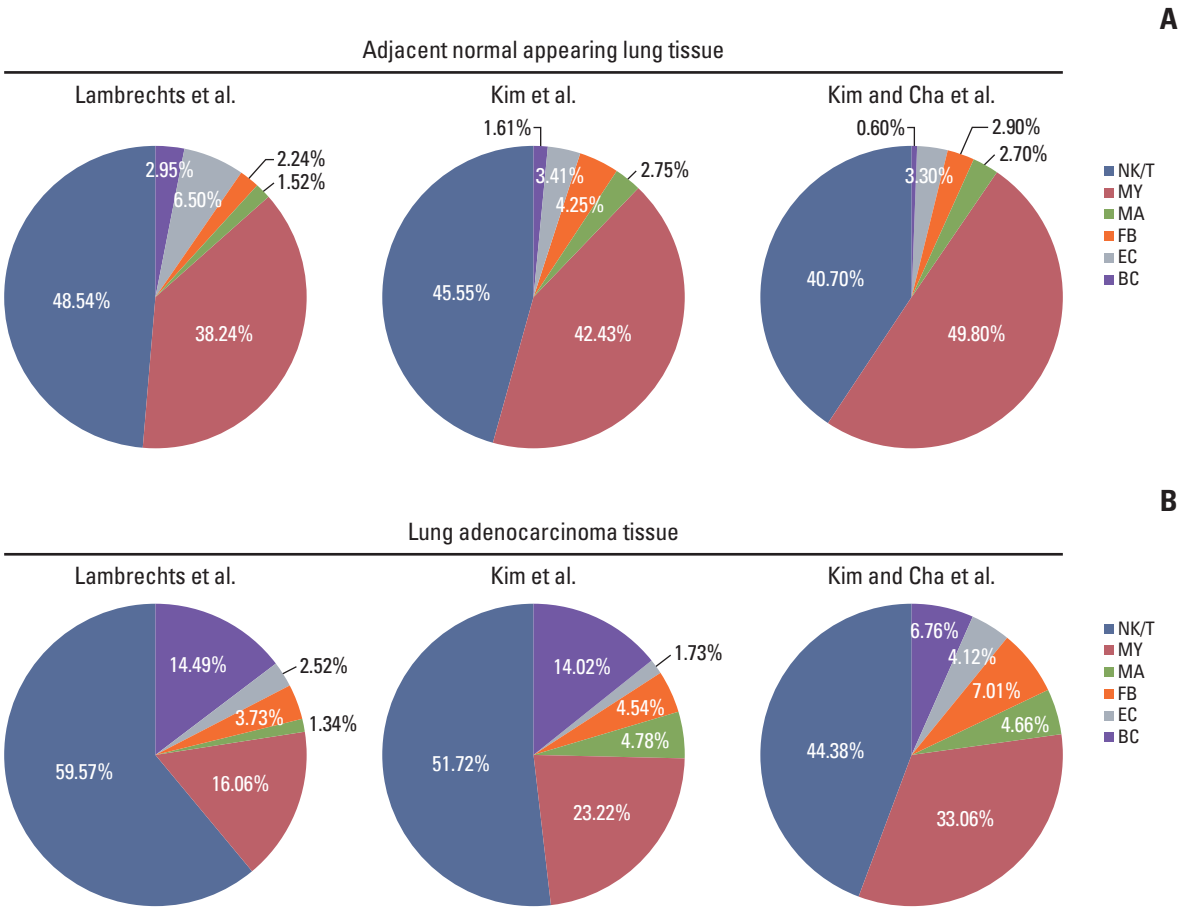

Fig. 1. Among the myeloid cells (MY) subclusters, those increased in tumor (Tu) showed overexpression triggering receptor expressed on myeloid cells 2 (*TREM2*). (A) Pie charts showing the proportions of major cell clusters in normal-appearing adjacent lung tissue (NL). (B) Pie charts depicting the cell cluster fractions in the tumor microenvironment of lung adenocarcinoma (Tu) corresponding to dataset used in (A). The fractions were estimated using datasets from our research team [10,15] and publicly available single-cell RNA sequencing datasets [8,9]. Note that cancer and epithelial cells, which vary widely based on tumor invasion degree, were excluded from the fraction calculations. BC, B cells; DC, dendritic cell; EC, endothelial cells; FB, fibroblasts; LC, Langerhans cell; Mac/Mc, macrophage; MA, mast cells; Mo, monocyte; NK/T, natural killer and T cells; pDC, plasmacytoid dendritic cell. *(Continued to the next page)*

Sigma-Aldrich) beads or 40 μL/mL fluorescent yellow-green beads were selected according to the fluorescent combination, added to the media, and cultured for 24 hours before being fixed and stained. Drug concentrations were determined based on previous studies within ranges that do not affect cell viability [12,13].

5. Analysis of IF staining

The M1 and M2 fractions of the Tu and NL were obtained by normalizing the number of CD86+ and CD163+ cells to the number of CD68+ cells in the corresponding area. For IF staining, QuPath software ver. 0.5.0 was used to measure the co-expression of biomarkers. Briefly, the images to be analyzed were imported into one project, and independent annotation areas within each image were defined. We first used the DAPI channel to detect all cells within a defined area. Thereafter, individual markers were measured for staining intensity, and a classifier was set up for each. The phagocytosis of PdSer-coated or uncoated latex beads within cells was measured using the subcellular spot detection function in QuPath. Spots showing values greater than 1.6 times the representative value were designated as bead clusters. The number of beads phagocytosed within cells was estimated using the "Subcellular: Channel 2: Num spots estimated" value and analyzed.

6. Statistical analysis

The DEGs between the two clusters of interest were determined using the Wilcoxon rank-sum test, which is the default option in Seurat ver. 4.4, and adjusted p-values were

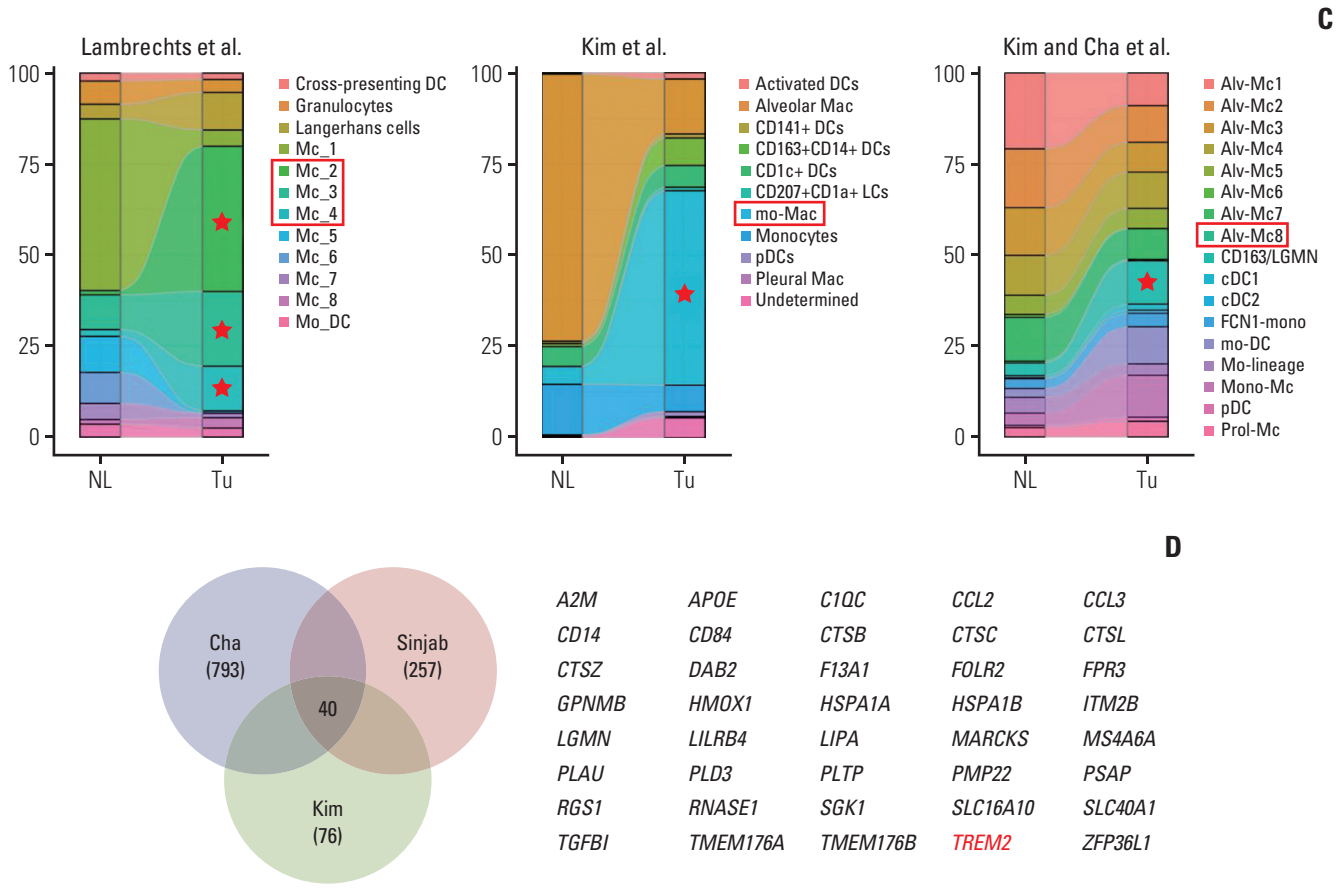

Fig. 1. *(Continued from the previous page)* (C) Alluvial plots illustrating the distribution differences between NL and Tu after myeloid cell subclustering and annotation. Fraction of some myeloid cell subclusters increased in Tu compared to NL. Increased subclusters were marked with asterisks and boxes. The annotations of the subclusters were quoted from the original paper. (D) Venn diagram showing differentially expressed genes (DEGs) identified by comparing myeloid subclusters that showed an increase in Tu with the remaining subclusters in each of the three datasets, and the intersection of the DEG sets yielded a final set of 40 genes.

obtained using Bonferroni correction. Differences in distribution between NL and Tu in the cluster of interest were determined by dividing the number of cells belonging to individual subclusters by the total number of cells belonging to the subcluster of the corresponding case and compared using the unpaired Wilcoxon rank-sum test.

Results

1. Among the myeloid cells subclusters, those increased in Tu overexpress *TREM2*

We estimated the fractions of major cell populations in the NL and Tu using scRNA-seq datasets reported by Lambrechts et al. [8], Kim et al. [9], Sinjab et al. [14], Kim et al. [15], and Cha et al. [10]. Data analyses focused on the non-epithelial cell population in the NL and Tu, noting that the yield may vary depending on cancer cell prevalence in the Tu and sample processing during the scRNA-seq workflow. Myeloid cells (MY) constituted 33.8%-49.8% of the cell population in the NL, being the second-largest fraction after NK/T cells (Table 1, Fig. 1A). In the paired Tu–NL datasets, the myeloid fraction consistently decreased in the Tu compared to that in the NL across all datasets, ranging from −1.9% to −22.1% (Fig. 1B) [8,14].

By additionally analyzing published scRNA-seq datasets, we identified myeloid cell subclusters with a higher proportion in the Tu than that in the NL, despite an overall decrease in the myeloid fraction within the TME. Characteristically, these myeloid cell subclusters' fraction was relatively low in the NL but became predominant in the Tu (Fig. 1C) [8-10]. Comparing these cells to the remaining myeloid subclusters within each dataset generated three DEG lists, whose intersection resulted in 40 genes (Fig. 1D). *TREM2* was selected

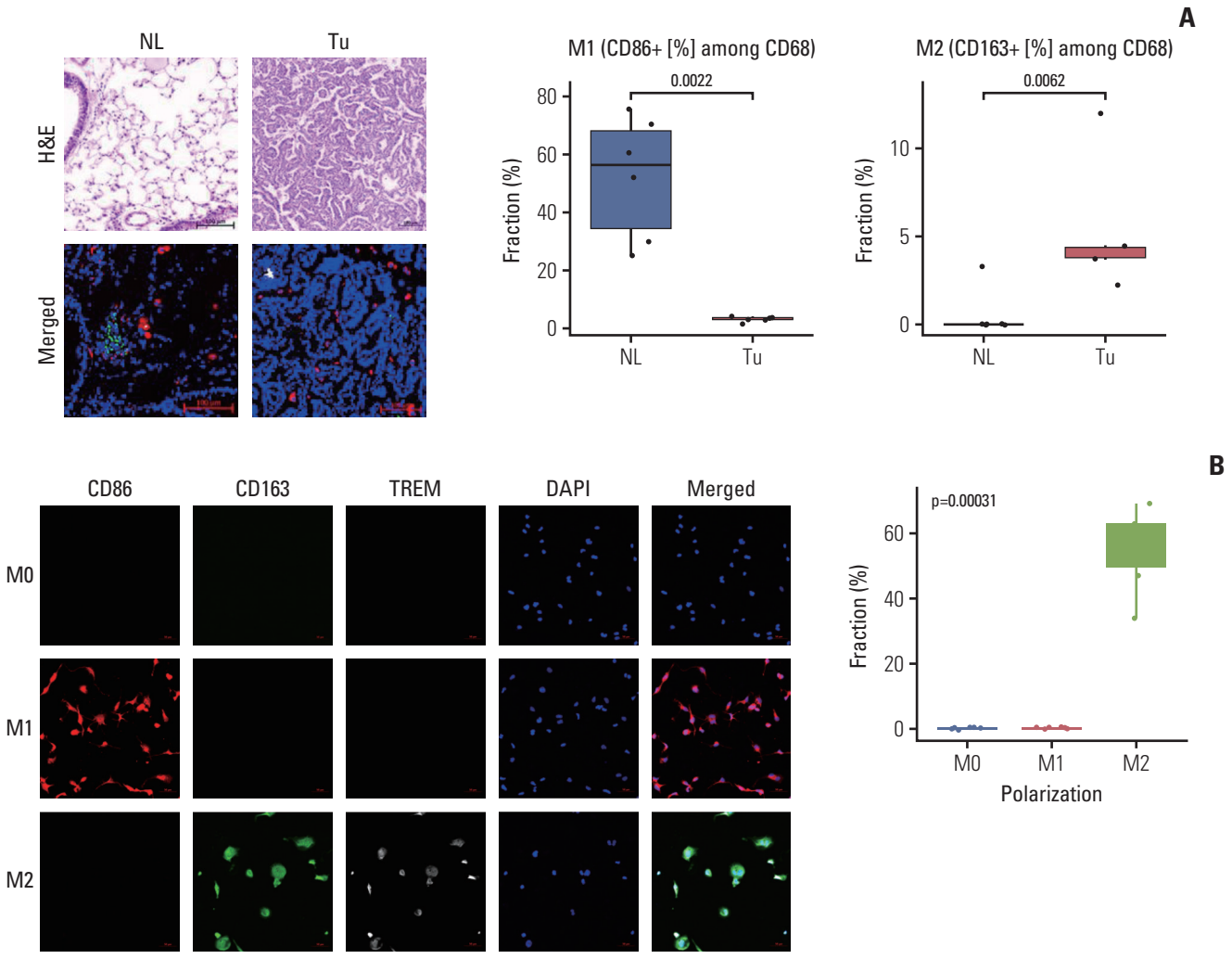

Fig. 2. Triggering receptor expressed on myeloid cells 2 (TREM2)+ cells with M2 features are increased in tumor (Tu). (A) Immunofluorescence (IF) staining for CD68 (red), CD86 (green), and CD163 (white) in normal-appearing lung tissue (NL) (left panel) and Tu (right panel) from a mouse lung cancer model, with corresponding hematoxylin and eosin (H&E) staining. Jittered box plots show the proportions of CD86+ and CD163+ cells among CD68+ mononuclear cells. p-values obtained via Kruskal-Wallis rank sum test. (B) IF staining for CD86 (red), CD163 (green), and TREM2 (white) in THP-1 cells polarized to M0, M1, and M2 states. Jittered box plot quantifying TREM2+ cell fraction among M0, M1, and M2. *(Continued to the next page)*

for further investigation among the 40 genes because it plays a role in clearing apoptotic cells via its extracellular domain [16], potentially influencing macrophages in the TME during anticancer therapy. In summary, although the total myeloid cell fraction of Tu was lower than that of NL, the myeloid cells overexpressing *TREM2* (hereinafter referred to as "TREM2+ cells") were increased in Tu.

2. TREM2+ cells with M2 features are increased in Tu

To explore the characteristics of TREM2+ cells distribution in NL and Tu, we used lung cancer tissues from mice and humans for TREM2 IHC, and THP-1 cells for *in vitro* analysis. First, to assess M1 and M2 distribution in the NL and Tu, IF staining with CD68, CD86, and CD163 was performed on Kras-G12D mouse lung cancer tissues. The results showed a high proportion of CD86+ cells (M1) in the NL, whereas CD163+ cells (M2) were prevalent in the Tu (Fig. 2A). Then, *in vitro* THP-1 cell polarization was utilized to explore the relationship between M2 macrophages and TREM2+ cells. Indeed, TREM2 overexpression was induced specifically in the M2 polarized state (Fig. 2B). IF, including TREM2 staining, revealed that a significant number of M2 macrophages were TREM2+. Notably, the proportion of TREM2+ M2 macrophages (TREM2+ CD163+) was significantly higher in Tu

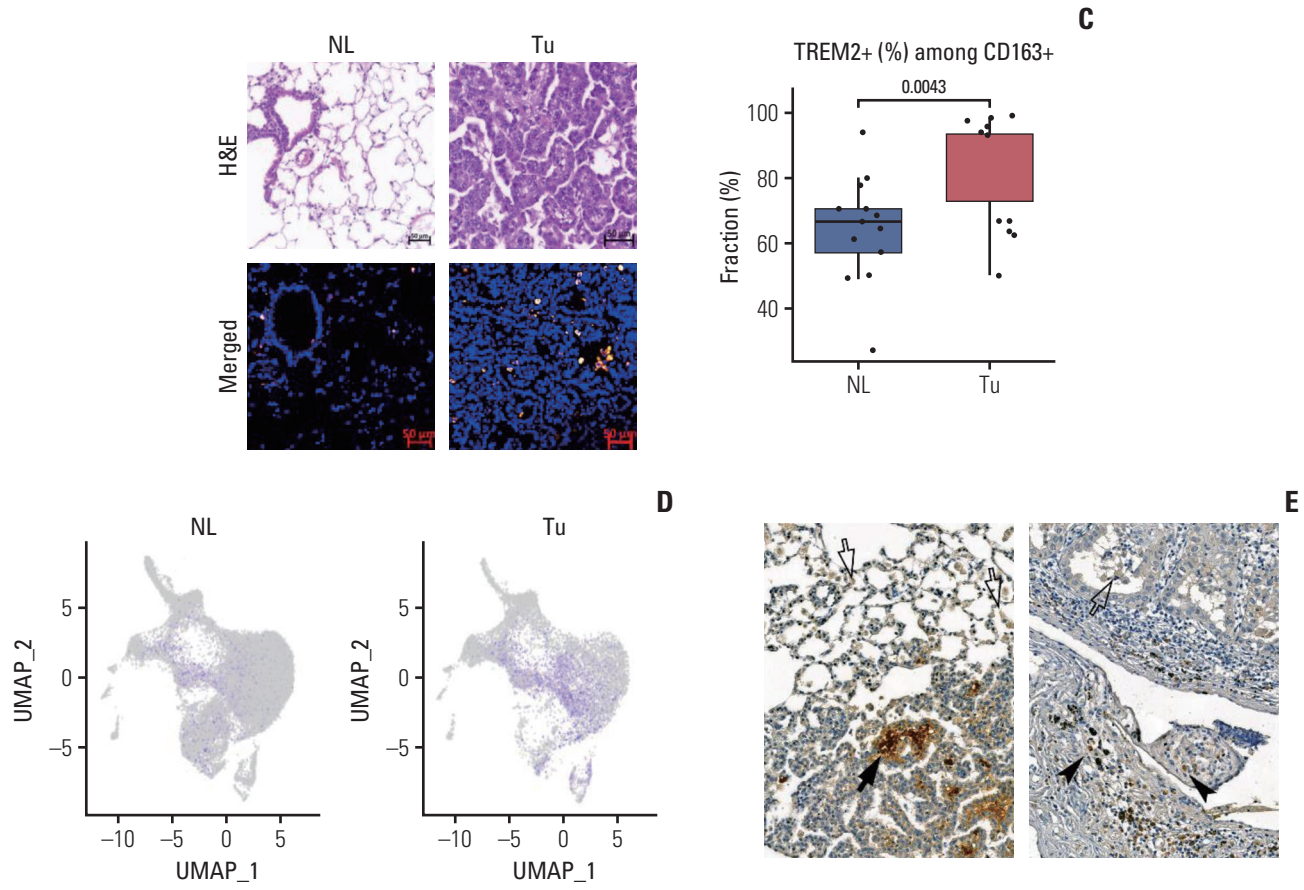

Fig. 2. *(Continued from the previous page)* (C) IF staining for CD68 (red), CD163 (green), and TREM2 (white) in NL (left panel) and Tu (right panel) from a mouse lung cancer model, with corresponding H&E staining. Jittered box plot shows the proportion of TREM2+ cells among CD163+ mononuclear cells by tissue type. p-value obtained via Kruskal-Wallis rank sum test. (D) Uniform Manifold Approximation and Projection plots showing *TREM2* expression in myeloid cells from normal-appearing adjacent lung tissue (NL) and tumor tissue (Tu). TREM2+ cells constitute 1,380 out of 11,669 (11.8%) myeloid cells in the Tu and 1,231 out of 35,035 (3.5%) myeloid cells in the NL (prop. test, $p < 0.001$). (E) TREM2 immunohistochemistry staining in mouse (left panel) and human (right panel) lung cancer tissues, highlighting TREM2 expression in tumor-associated macrophages (arrows) and absence in alveolar macrophages (empty arrows).

than that in NL (Fig. 2C). From the scRNA-seq dataset previously reported, we compared the distribution of TREM2+ cells with other myeloid cells in the Tu [10,15]. The TREM2+ cell proportion in the Tu (11.8%, 1,380/11,669 cells) was significantly higher than that in the NL (3.5%, 1,231/35,035 cells; $p < 0.001$) (Fig. 2D). In Kras-G12D mouse lung cancer tissues, TREM2 was expressed in TAMs. In human lung cancer tissues, TREM2 was not overexpressed in cancer cells or alveolar macrophages but in some interstitial mononuclear cells (Fig. 2E). Taken together, these results suggest that TREM2+ cells, which are relatively abundant in the Tu, exhibit M2-like traits.

3. Characteristics of TREM2+ cells and interactions with other MY subclusters implicates their role in immune evasion within Tu

Next, we analyzed the characteristics of gene expression in TREM2+ cells. From the scRNA-seq dataset previously reported, we compared the characteristics of TREM2+ and other myeloid cells in the Tu. These TREM2+ cells were distinct from alveolar macrophages owing to low *PPARG*, *FABP4*, and *CEBPB* expression. Additionally, *PLA2G7*, *PIGR*, *A2M*, and *LIPA*, which modulate and alleviate inflammation, and *A2M*, *MMP9*, and *SPP1*, which are involved in tissue repair and remodeling were overexpressed in these cells (Fig. 3A, S3 Table).

The DEGs obtained from comparison of TREM2+ cells with other myeloid cells in the Tu showed enrichment of genes

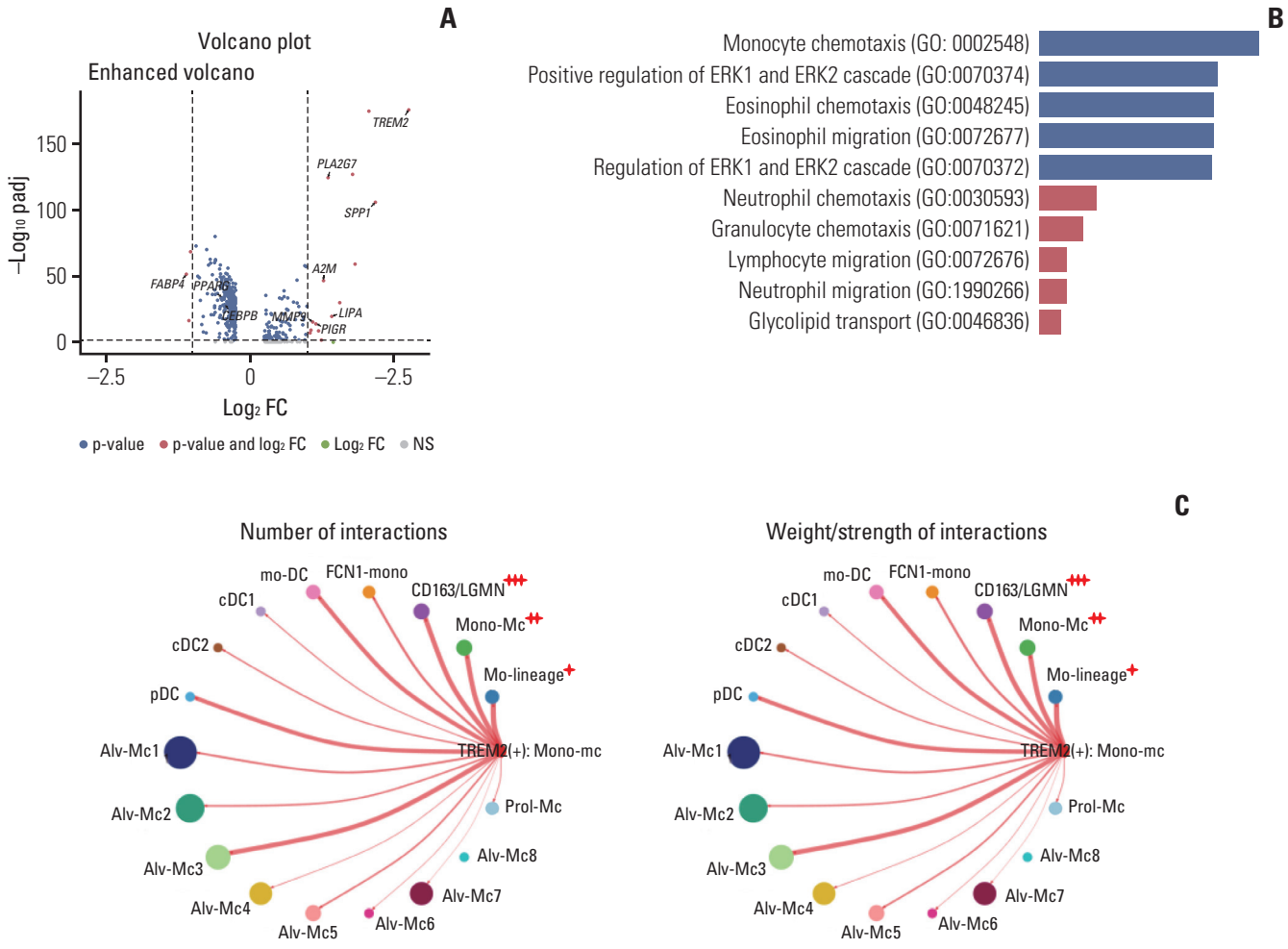

Fig. 3. Characteristics of triggering receptor expressed on myeloid cells 2 (TREM2)+ cells and interactions with other myeloid cells (MY) subclusters. (A) Volcano plot illustrating differentially expressed genes (DEGs) between TREM2+ cells and other MY subclusters in the tumor microenvironment (TME), based on single-cell RNA sequencing (scRNA-seq) data from Cha et al. [10]. (B) Clustergram of gene sets enriched in DEGs derived from the comparison of TREM2+ cells and other MY subclusters in the TME of lung cancer. It highlights significant enrichment of gene sets associated with chemotaxis and cell migration. Notably, these include pathways such as positive regulation of monocyte chemotaxis (GO:0090026) and regulation of monocyte chemotaxis (GO:0090025). For a detailed list, please refer to S3 Table. (C) Circular plots illustrating the number (left) and weight/strength (right) of interactions in the aggregated cell-cell communication network between TREM2+ cells and MY subclusters in the TME, generated using CellChat. Alv-Mc, alveolar macrophage; cDC, conventional dendritic cell; FC, fold change; Mo, monocyte; mono-Mc, monocyte-derived macrophage; NS, not significant; Prol-Mc, proliferating macrophage; pDC, plasmacytoid dendritic cell. *(Continued to the next page)*

associated with monocyte chemotaxis and migration (e.g., GO:0090025 and GO:0090026) (Fig. 3B). To further explore the role of TREM2+ cells in cell migration and tissue remodeling in the TME, we used CellChat to search for MY subclusters interacting in the TME. The MY subclusters, which was presumed to strongly interact with TREM2+ cells, were in the order Mono-lineage, Mono-Mc, and CD163/LGMN, which shows the characteristics of bone marrow-derived macrophages (Fig. 3C). The interaction between TREM2+ cells and these cell clusters showed similar ligand–receptor interactions. The interaction *MIF:CD74* and its co-factor *CXCR4* is thought to be involved in the guiding and trafficking of the associated cell population to Tu [17,18], while the *FN1:CD44* interaction is thought to be involved in the movement of these cell populations to Tu through the organization of the cytoskeleton and Tu [19] (Fig. 3D).

In summary, TREM2+ cells, enriched within the Tu, alleviate inflammation and contribute to its remodeling. Additionally, they interact with Mono-lineage, Mono-Mc, and CD163/LGMN, facilitating the trafficking and migration of

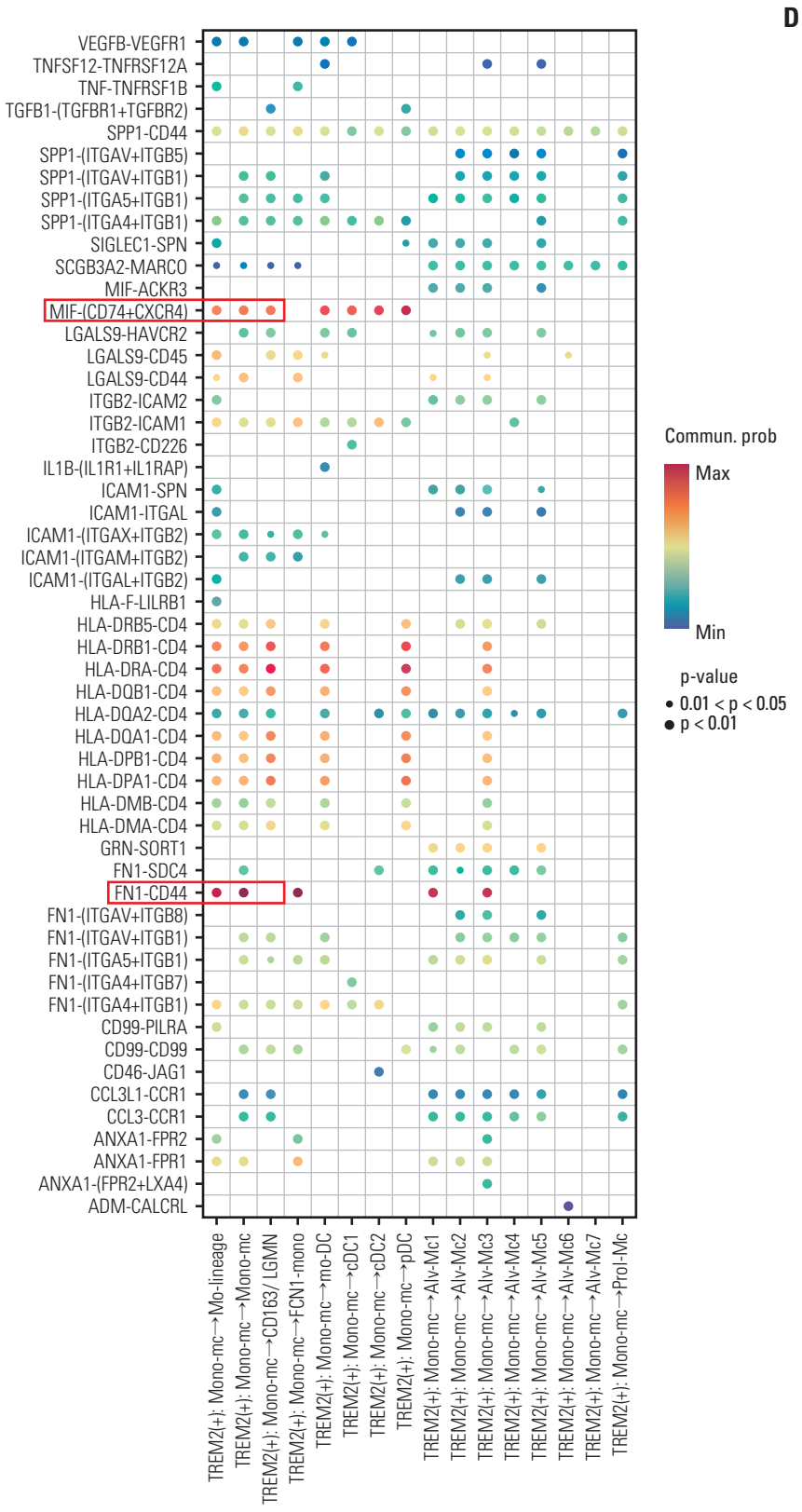

Fig. 3. *(Continued from the previous page)* (D) Bubble plot depicting individual interacting receptor-ligand pairs involved in cell-cell communication, with color indicating communication probability and bubble size representing p-values.

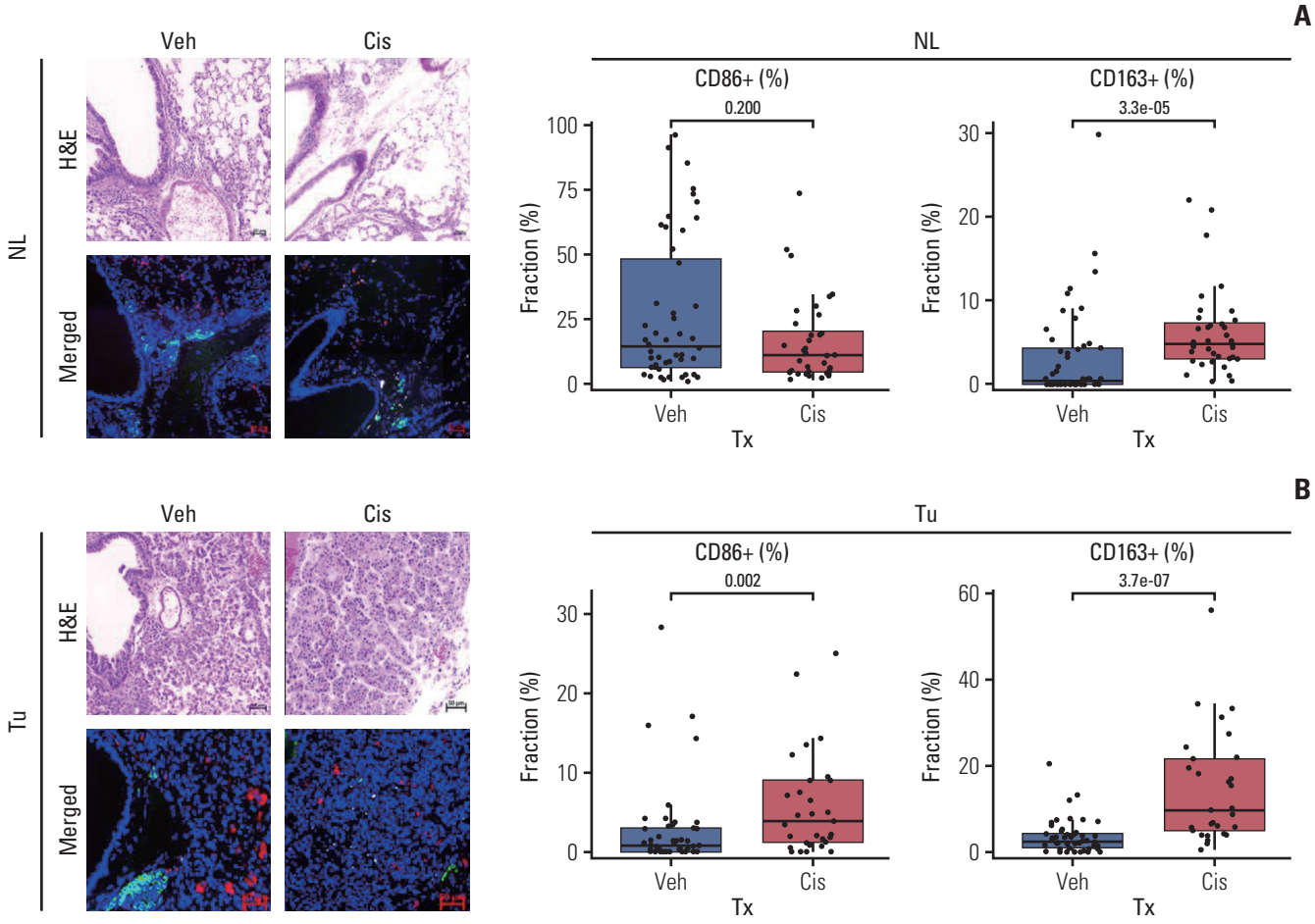

Fig. 4. Anticancer treatment promotes polarization into M1 and M2 and induces overexpression of triggering receptor expressed on myeloid cells 2 (TREM2). (A) Immunofluorescence (IF) staining for CD68 (red), CD86 (green), CD163 (white), and DAPI (blue) in normal-appearing adjacent lung tissue (NL) treated with vehicle (Veh) and cisplatin (Cis). Each IF image is accompanied by its corresponding hematoxylin and eosin (H&E)–stained section. Jittered box plots display the fraction of CD86+ (M1) and CD163+ (M2) mononuclear cells among CD68+ cells in NL tissues following treatment (Tx). p-value obtained via Kruskal-Wallis rank sum test. (B) Similar IF staining and analysis as in (A) but for tumor (Tu) tissue. *(Continued to the next page)*

these cell populations into Tu. Through these interactions, TREM2+ cells may play a pivotal role in shaping the immunosuppressive environment characteristic of the TME.

4. Anticancer treatment promotes polarization and TREM2 overexpression

Then, we investigated the effect of anticancer treatment on the accumulation of TREM2+ cells, which is reported to be involved in the formation of an immunosuppressive TME of the lung. First, we observed the effect of anticancer treatment on the distribution of M1 and M2 in NL and Tu. For this, we measured the ratios of CD86+ M1 and CD163+ M2 macrophages among CD68+ macrophages in NL (Fig. 4A) and Tu of Kras-G12D mouse lung cancer tissues (Fig. 4B) with and without cisplatin treatment. Following treatment with cisplatin, both M1 and M2 ratios increased, with a more pronounced increase in M2 macrophages.

Treatment with cisplatin or osimertinib, a third-generation EGFR–TKI, induced macrophage polarization and TREM2 expression in M0-state THP-1 cells. The polarized macrophage fraction significantly increased with anticancer treatment, becoming more pronounced over time. Furthermore, cytomorphologic metrics, specifically cell area, significantly increased after treatment (Fig. 4C). Collectively, these findings indicate that anticancer treatment induces the polarization of M0 state into M1 and/or M2 states. Furthermore, we observed the phenotypic change in various states of THP-1 cell-derived macrophages after treatment with anticancer drugs. In addition to M2, which showed overexpression of *TREM2*, both M0 and M1 states showed TREM2

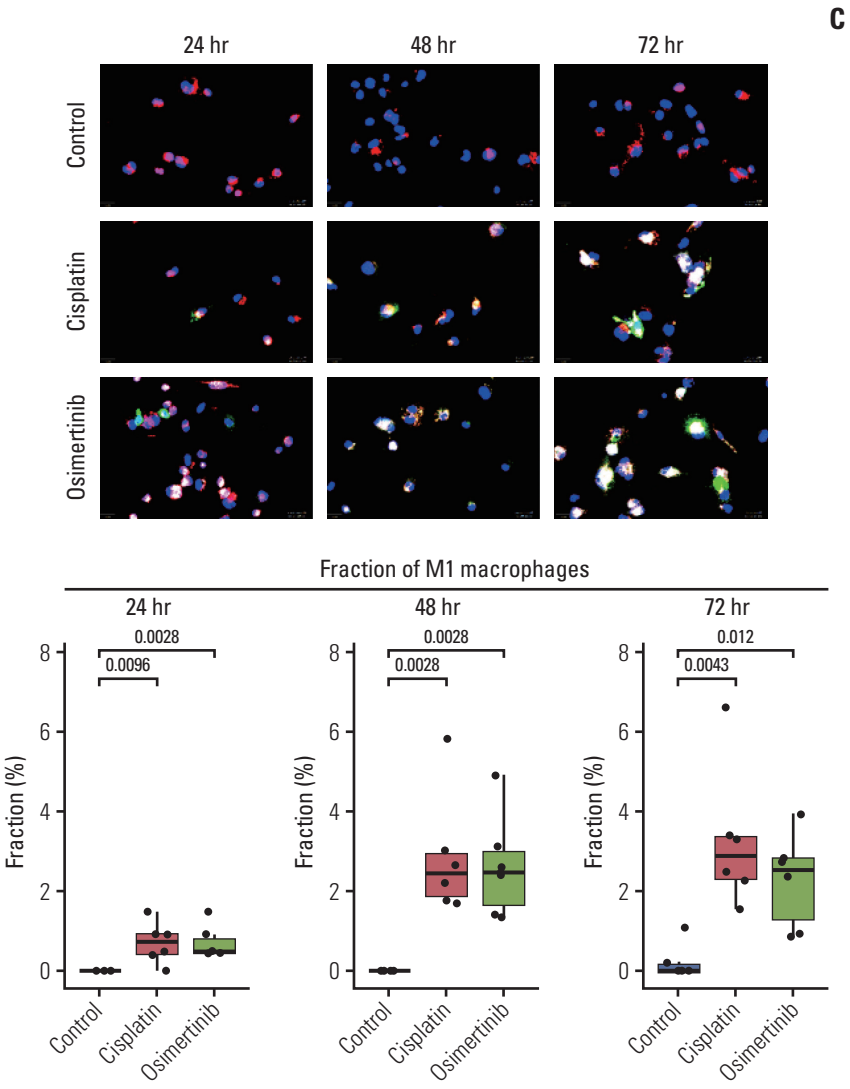

Fig. 4. *(Continued from the previous page)* (C) IF staining for CD68, CD86, and CD163 in THP-1 cells at the M0 state treated with 0.5 μM Cis and 100 nM osimertinib for indicated times. Jittered box plots depict the fractions of M1 and M2 macrophages and changes in cytomorphologic metrics over time. *(Continued to the next page)*

overexpression and cytomorphological changes after 24 hours after exposure to cisplatin and osimertinib (S4 Fig.). We further evaluated whether anticancer treatment affects TREM2 expression in NL and Tu cells from a Kras-G12D mouse lung cancer model. Cisplatin treatment did increase the fraction expressing TREM2+ cells among CD68 cells both in NL and Tu (Fig. 4D and E). Moreover, cisplatin induced robust expression of TREM2 (Fig. 4E). Taken together, these findings suggest that anticancer treatment could have a profound effect on macrophage polarization and change the TME into a more immunosuppressive environment.

5. Osimertinib inhibits the uptake of PdSer-coated latex beads by M1 and M2

Efferocytosis of apoptotic cell debris by macrophages is crucial in establishing an immune suppressive environment in the Tu by releasing anti-inflammatory or immunosuppressive signals, with *TREM2* presumed to be central in this process [1,20]. To simulate the effects of anticancer therapy on the efferocytosis of polarized macrophages, 2 μm diameter PdSer-coated latex beads were added to the culture medium of differentiating macrophages for 24 hours. As a control, uncoated latex beads were added to the medium of THP-1 cells polarized into the M0, M1, and M2 states. After 24 hours, approximately 1-2 beads per cell were observed

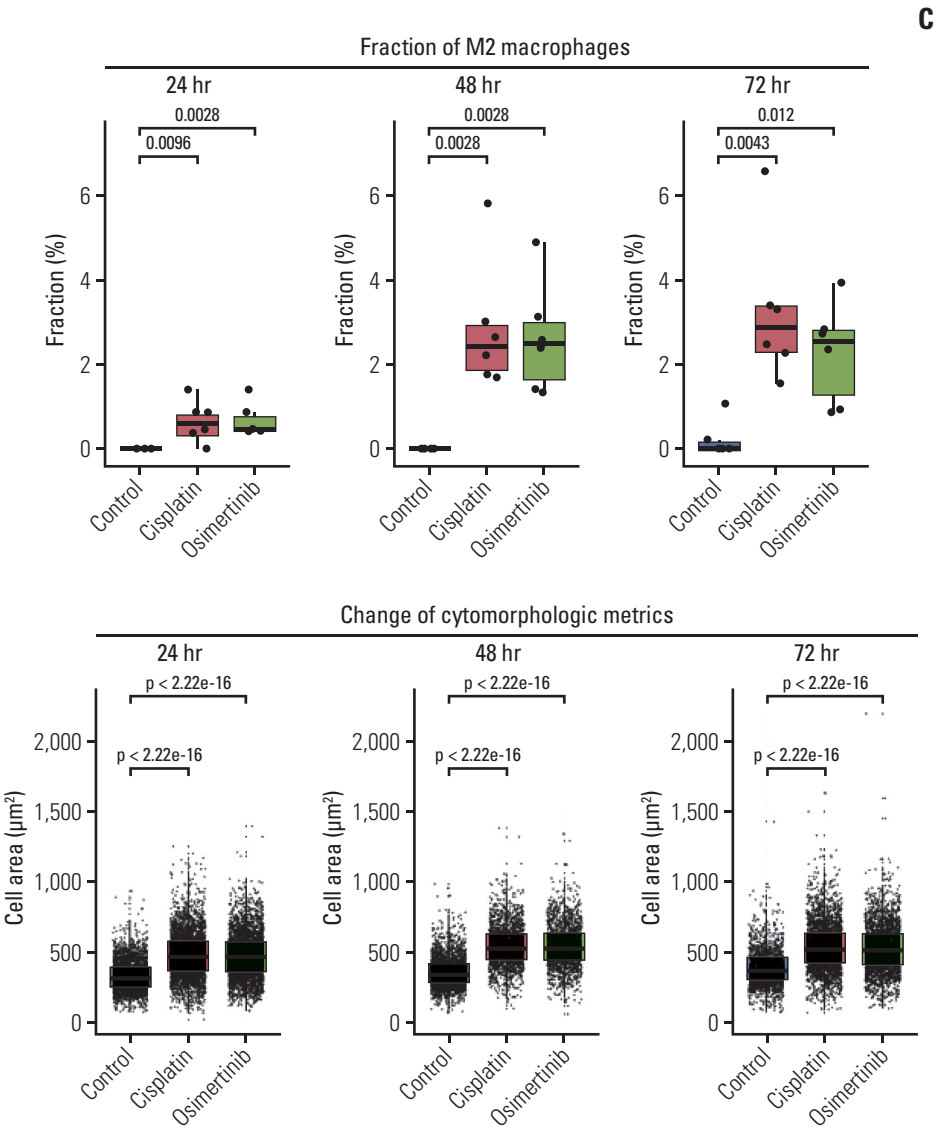

Fig. 4. *(Continued from the previous page) (Continued to the next page)*

within the cytoplasm (S5 Fig.). Meanwhile, the uptake of PdSer-coated latex beads differed significantly depending on the macrophage polarization state. Without treatment, M1 macrophages engulfed an average of 2.5 beads per cell, whereas M2 macrophages internalized 7.5 beads per cell, which indicates that the polarization state profoundly affects phagocytic activity (Fig. 5A and B). Within each polarization state, the impact of anticancer treatments on phagocytic activity differed. Osimertinib, a third-generation EGFR-TKI, treatment reduced bead uptake in both M1 and M2 macrophages, while cisplatin treatment had no effect on bead uptake in either state. To further investigate the role of TREM2 in macrophage-mediated phagocytosis, we utilized *TREM2* knockout (*TREM2* KO) THP-1 cells generated using CRISPR/Cas9 (S6A Fig.). The knockout of *TREM2* did not significantly affect the uptake of PdSer-coated latex beads by polarized M1 and M2 macrophages compared to wild-type cells (S6B and C Fig.). These findings suggest that phagocytic activity in polarized macrophages may be regulated through TREM2-independent pathways or compensatory mechanisms.

In summary, the anticancer agents, cisplatin and osimertinib, promoted differentiation towards the M2 phenotype and significantly upregulated TREM2 expression. However, neither drug facilitated the uptake of PdSer-coated latex beads in the polarized macrophages. Notably, osimertinib, a third-generation EGFR-TKI, inhibited bead uptake.

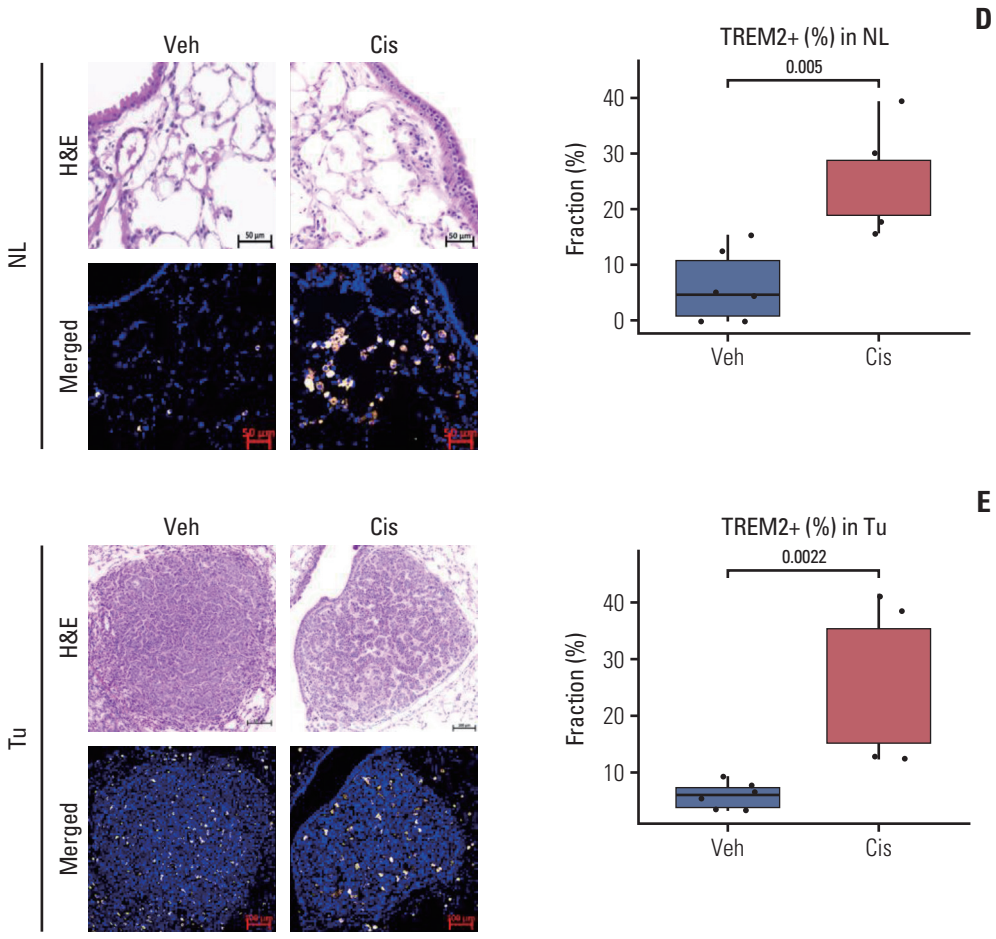

Fig. 4. *(Continued from the previous page)* (D) IF staining showing TREM2+ cells in NL tissues following treatment with vehicle and Cis. Each IF image is accompanied by its corresponding H&E-stained section. Corresponding jittered box plot shows the fraction of TREM2+ cells among CD68+ mononuclear cells. p-value obtained via Kruskal-Wallis rank sum test. (E) Similar IF staining and analysis as in (D) but for tumor tissue.

Discussion

In this study, we explored the influence of antitumor treatments on macrophages, their phenotype, and *TREM2* status. Our result aligned with previous findings that the proportion of TREM2+ M2 macrophages was higher in the Tu than that in the NL [2,21,22]. Moreover, we observed that M2 polarization can induce TREM2 expression in macrophages. Interestingly, both cisplatin and osimertinib treatment induced macrophage polarization into M1 or M2 states. Anticancer drug-induced overexpression of *TREM2* did not lead to increased uptake of phosphatidylserine-coated latex beads. Rather, the EGFR-TKI osimertinib inhibited uptake of PdSer-coated latex beads in M1 and M2 polarized macrophages.

The human *TREM* gene family, located on chromosome 6p21.1, shares structural similarities with the mouse *TREM* gene cluster on chromosome 17, which includes *TREM1*, *TREM2*, *TREML2*, and *TREML4* [23]. *TREM2* involvement in neurodegenerative diseases, particularly Alzheimer's disease (AD), has been extensively studied [24,25], where TREM2 overexpression may enhance the phagocytic activity of microglia [26]. In tumors, *TREM2* modulates macrophage [27], efficiently clearing particles coated with *TREM2* ligands, such as cellular debris displaying PdSer [1,28].

PdSer-mediated apoptotic cell uptake and clearance involve key receptors such as Cd300lb, *TIMD4*, and *MERTK*, which are critical for maintaining tissue homeostasis and resolving inflammation [24,29-31]. *TREM2* is known to be expressed in human microglia, osteoclasts, and tissue-resident macrophages, hypothesized to recognize phospholipids and sulfides exposed on apoptotic cells [32]. In our study, using PdSer-coated latex beads, the impact of *TREM2*, that was induced by anticancer treatment, on lipid binding or uptake was not clearly defined. In addition to the TREM2

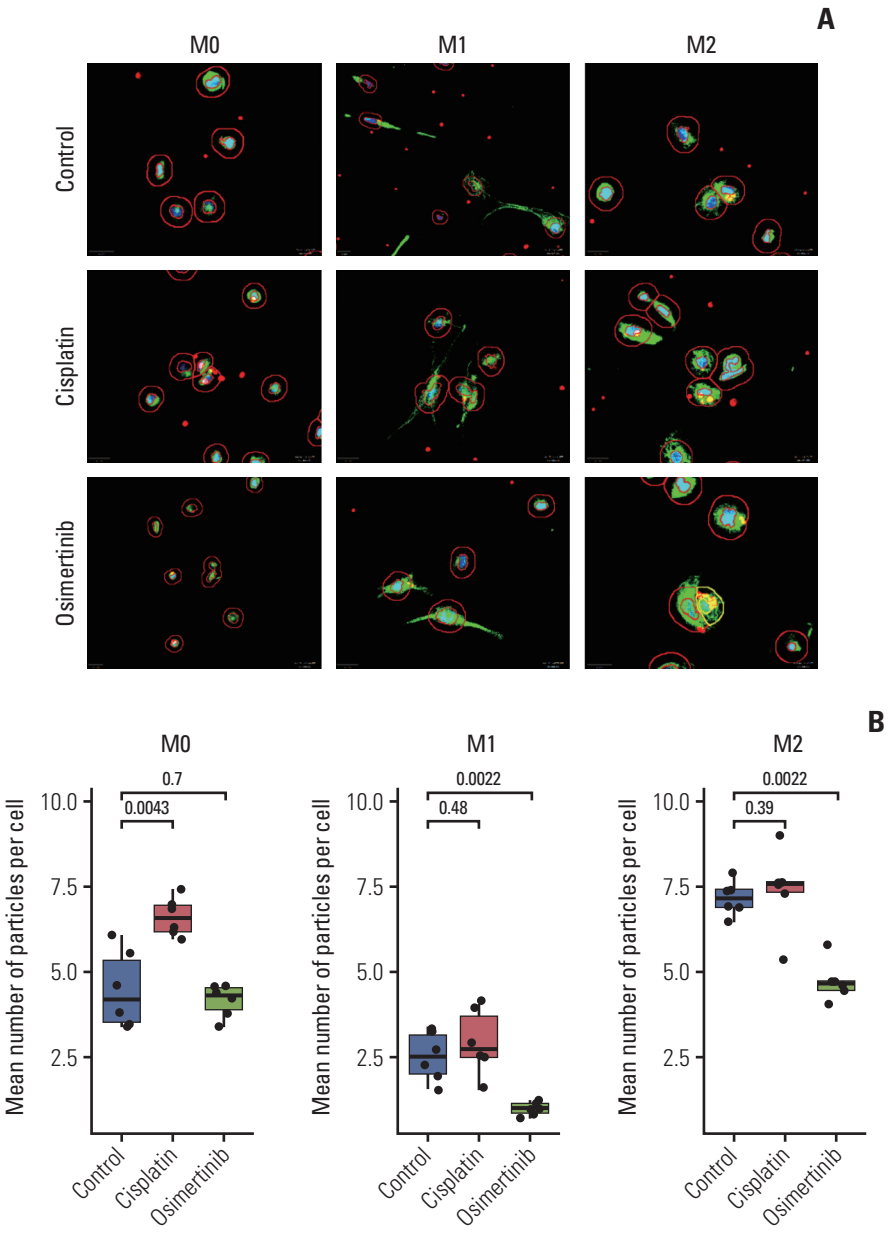

Fig. 5. Osimertinib inhibits the uptake of phosphatidylserine (PdSer)-coated latex beads by M1 and M2. (A) Immunofluorescence staining showing the impact of 0.5 μM cisplatin or 100 nM osimertinib on the PdSer-coated latex beads uptake of THP-1 cells polarized to M1, and M2 states. (B) Box plots illustrate the mean number of beads per cell, quantified using QuPath.

expression in different macrophage states, anticancer treatment appeared to modulate TREM2 expression and functional state of macrophages.

Interestingly, our findings from *TREM2* knockout (*TREM2* KO) THP-1 cells revealed that the loss of *TREM2* did not significantly affect the phagocytic activity of polarized macrophages. This suggests that other pathways or receptors may compensate for the absence of *TREM2* in mediating PdSer uptake. As has been well-documented, the Tyro3/Axl/Mer (TAM) receptor complex plays a central role in the clearance of apoptotic bodies, including those coated with phosphatidylserine [33,34]. Therefore, it is plausible that in the absence of TREM2, the TAM receptor complex could mediate the observed phagocytic activity in PdSer-coated bead uptake.

Studies on THP-1 cells have shown that M1 polarization reduces phagocytic activity compared to M0, while M2 polarization increases it, consistent with our findings [35].

However, contrasting results have been reported [36], likely influenced by the type of phagocytosis-triggering agent, such as apoptotic cells or specific pathogens. In the control group, phagocytic activity was most profound in TREM2+ M2 macrophages with PdSer-coated latex beads. Cisplatin-treated TREM2+ M2 macrophages retained their phagocytic activity, whereas osimertinib-treated M1 and M2 polarized macrophages lost their phagocytic activity. This discrepancy likely stems from the distinct mechanisms of action of the two anticancer agents. Cisplatin, a conventional cytotoxic agent, targets proliferating cells, causing DNA damage, and induces apoptosis [37]. In contrast, the EGFR–TKI osimertinib irreversibly inhibits EGFR function and induces apoptosis [38]. Unlike cancer cells, macrophages are not highly proliferative, which may explain their resilience to cisplatin. Furthermore, because EGFR is naturally expressed in macrophages and involved in modulating immune responses [39], osimertinib treatment could have reduced both the phagocytic activity and the effect of *TREM2* in macrophages.

TREM2 expression in various solid tumors is either positively or negatively correlated with patient survival [40]. Moreover, reports on the clinical implications of TREM2 expression in non-small cell lung cancer cells themselves are very limited. Cheng et al. [40] reported that TREM2 overexpression in lung adenocarcinoma was associated with prolonged overall survival. In addition to the clinical implications of TREM2 overexpression in lung cancer cells, investigating the dynamics of TREM2 expression at both primary and metastatic sites, as well as in lung cancer cells and TAMs before and after treatment with immune checkpoint inhibitors (ICIs), will provide valuable insights into changes in the immune activity of the tumor microenvironment. These observations may further inform the development of novel therapeutic strategies. We assessed the clinical impact of TREM2 overexpression on prognosis using The Cancer Genome Atlas Lung Adenocarcinoma (TCGA-LUAD) dataset. On analyzing clinicopathological parameters such as tumor size, stage, age, smoking history, and RNA-seq data, we found that clinicopathological factors were not significantly related with TREM2 expression (data not shown). When the effect of TREM2 overexpression on the prognosis in patients from the TCGA-LUAD cohort was analyzed, this significance was lost after propensity-matched analysis in our study, which accounted for stage, age, sex, and smoking history (S7 Fig.). Interestingly, when TCGA-LUAD cases were categorized into quartiles based on tumor mutation burden (TMB), cases with the highest TMB (Q4) exhibited lower TREM2 expression than those with the lowest TMB (Q1) (data not shown). *TREM2* expression inversely correlated with TMB, which was also observed in a previous study [40]. Because a high TMB in lung cancer is a predictive factor for a good response to ICIs, *TREM2* overexpression might suggest a poor response to ICIs.

Our study has certain limitations. The effects of anticancer drugs on the phagocytic activity of polarized macrophages were assessed using *in vitro* experiments with a single cell line and PdSer-coated latex beads, which do not fully replicate the TME and the subsequent tumor-immune interactions. Additionally, further *in vivo* studies using TREM2-targeting drugs or TREM2 overexpressing or knockdown engineered models could not be performed. Lastly, the effects of osimertinib on myeloid cells *in vivo* remain unexplored due to its limited use as neoadjuvant chemotherapy, restricting access to human-derived samples.

Despite the limitations identified, this study provides robust evidence for the impact of cytotoxic and targeted cancer therapies on the phenotypic state and functional activities of macrophages. As the treatment landscape for lung cancer broadens to include immunotherapy, chemotherapy, and targeted therapy, selecting patients who are most likely to benefit from specific treatments has become increasingly critical. The TME is a pivotal factor influencing the biological behavior of tumors and may augment or mitigate the effects of therapeutic agents, depending on their mechanisms of action. *TREM2* is an immunosuppressive regulator within the myeloid subsets of the TME; however, its role in reshaping the immune environment under various treatments remains to be elucidated. Further *in vivo* and clinical studies are necessary to explore and validate the effects of *TREM2* modulation.

Electronic Supplementary Material

Supplementary materials are available at Cancer Research and Treatment website (https://www.e-crt.org).

Ethical Statement

This study was approved by the Institutional Review Board of Gangnam Severance Hospital (IRB No. 3-2024-0207) and was conducted in accordance with the principles of the Declaration of Helsinki. The requirement for informed consent was waived by the IRB of Gangnam Severance Hospital because human tissues were randomly extracted from de-identified tissue archives of non-small cell lung cancer. Mouse lung cancer tissues were obtained from the residual blocks of previous studies which had been approved by the IACUC, Yonsei Biomedical Research Institute, Yonsei University College of Medicine (2015-0307), and followed the American Association for the Assessment and Accreditation of Laboratory Animal Care guidelines.

Author Contributions

Conceived and designed the analysis: Chang YS.
Collected the data: Cha YJ, Lee EH, Park MK, Chang YS.

Contributed data or analysis tools: Cha YJ, Lee EH, Kim CY, Choi YJ, Park MK, Lee SH, Kim EY, Chang YS.
Performed the analysis: Cha YJ, Lee EH, Park MK, Chang YS.
Wrote the paper: Cha YJ, Lee EH, Chang YS.

ORCID iDs
Yoon Jin Cha : https://orcid.org/0000-0002-5967-4064
Eun Hye Lee : https://orcid.org/0000-0003-2570-3442
Yoon Soo Chang : https://orcid.org/0000-0003-3340-4223

Conflicts of Interest
Conflict of interest relevant to this article was not reported.

Funding
This study was supported by NRF-2023R1A2C1003235 awarded to YS Chang.

References

1. Deczkowska A, Weiner A, Amit I. The physiology, pathology, and potential therapeutic applications of the TREM2 signaling pathway. Cell. 2020;181:1207-17.
2. Park MD, Reyes-Torres I, LeBerichel J, Hamon P, LaMarche NM, Hegde S, et al. TREM2 macrophages drive NK cell paucity and dysfunction in lung cancer. Nat Immunol. 2023;24:792-801.
3. Han B, Jin B, Chu T, Niu Y, Dong Y, Xu J, et al. Combination of chemotherapy and gefitinib as first-line treatment for patients with advanced lung adenocarcinoma and sensitive EGFR mutations: a randomized controlled trial. Int J Cancer. 2017;141:1249-56.
4. Hosomi Y, Morita S, Sugawara S, Kato T, Fukuhara T, Gemma A, et al. Gefitinib alone versus gefitinib plus chemotherapy for non-small-cell lung cancer with mutated epidermal growth factor receptor: NEJ009 study. J Clin Oncol. 2020;38:115-23.
5. Miyauchi E, Morita S, Nakamura A, Hosomi Y, Watanabe K, Ikeda S, et al. Updated analysis of NEJ009: gefitinib-alone versus gefitinib plus chemotherapy for non-small-cell lung cancer with mutated EGFR. J Clin Oncol. 2022;40:3587-92.
6. Noronha V, Patil VM, Joshi A, Menon N, Chougule A, Mahajan A, et al. Gefitinib versus gefitinib plus pemetrexed and carboplatin chemotherapy in EGFR-mutated lung cancer. J Clin Oncol. 2020;38:124-36.
7. Planchard D, Janne PA, Cheng Y, Yang JC, Yanagitani N, Kim SW, et al. Osimertinib with or without chemotherapy in EGFR-mutated advanced NSCLC. N Engl J Med. 2023;389:1935-48.
8. Lambrechts D, Wauters E, Boeckx B, Aibar S, Nittner D, Burton O, et al. Phenotype molding of stromal cells in the lung tumor microenvironment. Nat Med. 2018;24:1277-89.
9. Kim N, Kim HK, Lee K, Hong Y, Cho JH, Choi JW, et al. Single-cell RNA sequencing demonstrates the molecular and cellular reprogramming of metastatic lung adenocarcinoma. Nat Commun. 2020;11:2285.
10. Cha YJ, Kim EY, Choi YJ, Kim CY, Park MK, Chang YS. Accumulation of plasmacytoid dendritic cell is associated with a treatment response to DNA-damaging treatment and favorable prognosis in lung adenocarcinoma. Front Immunol. 2023;14:1154881.
11. Genin M, Clement F, Fattaccioli A, Raes M, Michiels C. M1 and M2 macrophages derived from THP-1 cells differentially modulate the response of cancer cells to etoposide. BMC Cancer. 2015;15:577.
12. Kobyakova M, Lomovskaya Y, Senotov A, Lomovsky A, Minaychev V, Fadeeva I, et al. The increase in the drug resistance of acute myeloid leukemia THP-1 cells in high-density cell culture is associated with inflammatory-like activation and anti-apoptotic Bcl-2 proteins. Int J Mol Sci. 2022;23:7881.
13. Butterworth S, Finlay MR, Ward RA, Kadambar VK, Chandrashekar RC, Murugan A, et al. 2-(2,4,5-substituted-anilino) pyrimidine derivatives as EGFR modulators useful for treating cancer. Patent WO 2013014448A1. 2012.
14. Sinjab A, Han G, Treekitkarnmongkol W, Hara K, Brennan PM, Dang M, et al. Resolving the spatial and cellular architecture of lung adenocarcinoma by multiregion single-cell sequencing. Cancer Discov. 2021;11:2506-23.
15. Kim EY, Cha YJ, Lee SH, Jeong S, Choi YJ, Moon DH, et al. Early lung carcinogenesis and tumor microenvironment observed by single-cell transcriptome analysis. Transl Oncol. 2022;15:101277.
16. Colonna M, Wang Y. TREM2 variants: new keys to decipher Alzheimer disease pathogenesis. Nat Rev Neurosci. 2016;17:201-7.
17. Leng L, Metz CN, Fang Y, Xu J, Donnelly S, Baugh J, et al. MIF signal transduction initiated by binding to CD74. J Exp Med. 2003;197:1467-76.
18. Schwartz V, Lue H, Kraemer S, Korbiel J, Krohn R, Ohl K, et al. A functional heteromeric MIF receptor formed by CD74 and CXCR4. FEBS Lett. 2009;583:2749-57.
19. Spada S, Tocci A, Di Modugno F, Nistico P. Fibronectin as a multiregulatory molecule crucial in tumor matrisome: from structural and functional features to clinical practice in oncology. J Exp Clin Cancer Res. 2021;40:102.
20. Kober DL, Brett TJ. TREM2-ligand interactions in health and disease. J Mol Biol. 2017;429:1607-29.
21. Lavin Y, Kobayashi S, Leader A, Amir ED, Elefant N, Bigenwald C, et al. Innate immune landscape in early lung adenocarcinoma by paired single-cell analyses. Cell. 2017;169:750-65.
22. Cambier CJ, Takaki KK, Larson RP, Hernandez RE, Tobin DM, Urdahl KB, et al. Mycobacteria manipulate macrophage recruitment through coordinated use of membrane lipids.

Nature. 2014;505:218-22.
23. Colonna M. The biology of TREM receptors. Nat Rev Immunol. 2023;23:580-94.
24. Kleinberger G, Yamanishi Y, Suarez-Calvet M, Czirr E, Lohmann E, Cuyvers E, et al. TREM2 mutations implicated in neurodegeneration impair cell surface transport and phagocytosis. Sci Transl Med. 2014;6:243ra86.
25. Akhter R, Shao Y, Formica S, Khrestian M, Bekris LM. TREM2 alters the phagocytic, apoptotic and inflammatory response to Abeta(42) in HMC3 cells. Mol Immunol. 2021;131:171-9.
26. Li Y, Xu H, Wang H, Yang K, Luan J, Wang S. TREM2: potential therapeutic targeting of microglia for Alzheimer's disease. Biomed Pharmacother. 2023;165:115218.
27. Molgora M, Liu YA, Colonna M, Cella M. TREM2: a new player in the tumor microenvironment. Semin Immunol. 2023;67: 101739.
28. Yeh FL, Wang Y, Tom I, Gonzalez LC, Sheng M. TREM2 binds to apolipoproteins, including APOE and CLU/APOJ, and thereby facilitates uptake of amyloid-beta by microglia. Neuron. 2016;91:328-40.
29. Abbas AK, Lichtman AH, Pillai S. Cellular and molecular immunology. 10th ed. Elsevier; 2022.
30. Miyanishi M, Tada K, Koike M, Uchiyama Y, Kitamura T, Nagata S. Identification of Tim4 as a phosphatidylserine receptor. Nature. 2007;450:435-9.
31. Dransfield I, Zagorska A, Lew ED, Michail K, Lemke G. Mer receptor tyrosine kinase mediates both tethering and phagocytosis of apoptotic cells. Cell Death Dis. 2015;6:e1646.
32. Wang Y, Cella M, Mallinson K, Ulrich JD, Young KL, Robinette ML, et al. TREM2 lipid sensing sustains the microglial response in an Alzheimer's disease model. Cell. 2015;160:1061-71.
33. Lemke G, Rothlin CV. Immunobiology of the TAM receptors. Nat Rev Immunol. 2008;8:327-36.
34. Lemke G, Burstyn-Cohen T. TAM receptors and the clearance of apoptotic cells. Ann N Y Acad Sci. 2010;1209:23-9.
35. Mendoza-Coronel E, Ortega E. Macrophage polarization modulates FcgammaR- and CD13-mediated phagocytosis and reactive oxygen species production, independently of receptor membrane expression. Front Immunol. 2017;8:303.
36. Tedesco S, De Majo F, Kim J, Trenti A, Trevisi L, Fadini GP, et al. Convenience versus biological significance: are PMA-differentiated THP-1 cells a reliable substitute for blood-derived macrophages when studying in vitro polarization? Front Pharmacol. 2018;9:71.
37. Dasari S, Tchounwou PB. Cisplatin in cancer therapy: molecular mechanisms of action. Eur J Pharmacol. 2014;740:364-78.
38. Finlay MR, Anderton M, Ashton S, Ballard P, Bethel PA, Box MR, et al. Discovery of a potent and selective EGFR inhibitor (AZD9291) of both sensitizing and T790M resistance mutations that spares the wild type form of the receptor. J Med Chem. 2014;57:8249-67.
39. Hardbower DM, Singh K, Asim M, Verriere TG, Olivares-Villagomez D, Barry DP, et al. EGFR regulates macrophage activation and function in bacterial infection. J Clin Invest. 2016; 126:3296-312.
40. Cheng X, Wang X, Nie K, Cheng L, Zhang Z, Hu Y, et al. Systematic pan-cancer analysis identifies TREM2 as an immunological and prognostic biomarker. Front Immunol. 2021;12: 646523.